Journal of The Electrochemical Society, 2021 **168** 121507

Atomic Scale Insight into Corrosion Inhibition: DFT Study of 2-Mercaptobenzimidazole on Locally De-Passivated Copper Surfaces

Fatah Chiter,[z] Dominique Costa, Vincent Maurice,[z] and Philippe Marcus[*,z]

PSL University, CNRS—Chimie ParisTech, Institut de Recherche de Chimie Paris/Physical Chemistry of Surfaces Group, 75005 Paris, France

A key factor for effective inhibition by organic molecules of the initiation of localized corrosion by pitting is their ability to form a protective organic film in locally de-passivated zones exposing the bare metal next to the oxide-covered surface. Herein, based on quantum chemical DFT calculations, we study the chemistry of the interface between 2-mercaptobenzimidazole (MBI) and a copper surface partially covered by a Cu_2O passive oxide film. The results show the adaptability of the molecule to adsorb strongly on the different zones, oxide or metal, of a locally de-passivated surface. However, differences in the local adsorption configurations, involving covalent bonding with H-bonding depending on oxide or metal and on conformer, thione or thiolate, lead to the formation of an inhomogeneous organic film. Increasing order of local adsorption strength is oxide walls < metal surface < oxide surface < oxide edges for the thione species, whereas there is no significant difference of local adsorption strength for the thiolate species. Our results suggest that both species of MBI can heal the oxygen and copper low coordinated sites as well as can protect the exposed metal surface, thus enhancing the barrier properties of the passivated surface even when locally defective.
 [DOI: 10.1149/1945-7111/ac405c]

Manuscript submitted October 18, 2021; revised manuscript received November 25, 2021. Published December 16, 2021.

Corrosion inhibition by organic inhibitors depends on type of molecule, nature of the metal (alloy) and interfacial conditions as defined by surface state and corrosive environment. This complexity makes a deep understanding of the inhibition mechanisms a challenging task. Many works have been devoted to understand the corrosion inhibition effectiveness of various organic molecules in different experimental conditions, and also to investigate the surface chemistry of the molecule/metal (or alloy) interface by experimental and theoretical methods.[1–6] It is well established that what determines the effective corrosion inhibition of organic molecules is their ability to form a dense organic film on the metal surface. For that, the molecules must interact strongly with the substrate surface and self-assemble to form a stable and insoluble organic film. The organic film must have (physical and/or chemical) barrier properties against the ingress of aggressive reagents like chloride ions and must prevent the dissolution of the metal (or alloy) in the aqueous environment.

For copper, 2-mercaptobenzimidazole (MBI) molecule has been shown to exhibit high corrosion inhibition efficiency in different acidic aqueous media,[2–4,6,7] where it acts as a mixed type (anodic and cathodic) inhibitor with a stronger anodic effect.[3,4] For increasing immersion times (from few seconds up to 7 days), MBI forms thicker and more insulating organic films on copper in chloride (0.1 M KCl + 1 mM MBI) solution than in sodium sulfate (0.1 M Na_2SO_4 + 1 mM MBI) neutral solution.[8] MBI is also a good inhibitor for copper in neutral saline solutions[9,10] as well as in alkaline solution.[11] The inhibition efficiency of MBI on copper is comparable in acid and alkaline solutions[1,5,12,13] and is similar to that of 2-mercaptobenzothiazole (MBT).

Surface analytical studies have shown that MBI molecules self-assemble on oxidized or metallic copper surfaces and form a protective barrier against corrosion in various environments.[1,9,12] In aqueous environment, Chadwick and Hashemi[1] evidenced the formation of a protective film formed by MBI or MBT molecules on copper substrate under different conditions and suggested a precipitation mechanism for Cu_2-MBI film formation. The thickness of the protective organic layer would be controlled by the pH regime, which determines the stability domain of native Cu_2O oxide. The reaction products lead to the formation of an effective anti-corrosion film.[12] Several works suggested the formation of a continuous organo-metallic polymer (poly(MBI), Cu-MBI or Cu_2-MBI) on the copper surface.[1,10–13] Xue et al.[12] determined that the film forming on the metallic copper under mild conditions is different from that forming on the oxidized copper.[12] However, the film can subsequently act as protective barrier for copper exposed in acid, alkaline and aggressive environments, as determined by cyclic voltammetry.[12] When pre-adsorbed on the copper surface in metallic state, MBI blocks the growth of the Cu(I) surface oxide as observed in aqueous phase[14] as well as in the gas phase.[15] The investigation of the surface chemistry has shown that MBI interacts with copper via both nitrogen and sulfur atoms,[3,9,16] and Niamien et al.[17] suggested both physisorption and chemisorption interaction modes. In UHV condition,[15] MBI is chemisorbed via sulfur and the two nitrogen atoms when the molecule initially lies flat on the metallic copper surface and via S and one of the N atoms when in the tilted configuration at higher coverage.

Computational methods either following a standard Quantitative Structure Activity Relationship (QSAR) approach, or using the Density Functional Theory (DFT) and Molecular Dynamics (MD) frameworks bring relevant information on the corrosion inhibition properties of the molecules and are powerful for clarifying the nature of the adsorption of the molecule on the substrate surfaces. The methods are also used to compare the bonding strength of different molecules on the substrate surfaces and in correlation with the experimental inhibiting efficiency. For MBI, the corrosion inhibition properties were investigated relative to the electronic properties of the isolated molecule as a first indicator to describe its reactivity toward metals.[6,13,17,18]

The interfacial chemistry of MBI adsorbed on copper surfaces is well established using DFT and MD methods, especially regarding the nature of binding and the formation of organic layers on the surface. Sun et al.[19] found that at low coverage the thiolate form was strongly chemisorbed in both perpendicular and tilted adsorption configurations on the Cu(111) surface, whereas the thiol form was physisorbed or weakly chemisorbed in parallel or perpendicular configurations, respectively. The molecule was covalently bound through N–Cu and/or S–Cu bonds, which shows that both nitrogen and sulfur atoms are involved in the adsorption mechanism. The thione species also binds spontaneously to the Cu(111) surface, as well as to the Fe(110), Al(111) surfaces at low coverage in a parallel configuration via the S and N reactive sites and the π electrons.[20]

*Electrochemical Society Fellow.
[z]E-mail: fatah.chiter@chimieparistech.psl.eu; vincent.maurice@chimieparistech.psl.eu; philippe.marcus@chimieparistech.psl.eu

Other calculations confirmed that the thiol tautomers of mercapto molecules are less stable in gaseous as well as aqueous phases than the thione forms and that thione forms bond stronger to the copper surface.[20–22] It was also shown that the thiolate form binds to the Cu atoms via S and N atoms,[21,22] independently of the surface coverage.[22] The comparison of the chemisorption strength order of three potential inhibitors including MBI onto the clean Cu(111) surface is consistent with the experimental results of inhibiting efficiency.[19] The calculations also revealed that stand alone adsorbed molecules were thermodynamically more stable than organo-metallic adcomplexes on the Cu(111) surface. In contrast to other molecules, MBI molecules do not react with Cu^{2+} ions to form soluble complexes which would promote corrosion.[21]

These results are relevant to understand the reactivity of MBI and to describe the inhibitor-surface bonding on bare Cu(111) surfaces. In order to bring deeper insight of the surface chemistry of MBI adsorbed on copper, Chiter et al.[23] performed quantum chemical DFT calculations of the interaction mechanism of MBI in thione or thiolate forms at low and saturation coverage on a passivated Cu (111) surface, i.e. covered by an intact ultrathin Cu(I) oxide film (Cu (111)|| Cu_2O(111)). The thione species was found to interact strongly with the surface forming a S–Cu covalent bond and a H-bond with a surface oxygen atom, whereas the thiolate species formed two covalent S–Cu and N–Cu bonds, which increases the bonding strength. At saturation coverage, the molecules adopt a perpendicular configuration with respect to the surface, whereas at low coverage they tilt toward the surface.

Herein we report a quantum chemical DFT investigation of the different adsorption sites and adsorption configurations of the thione and thiolate species of MBI on a locally de-passivated copper surface. A model representing a Cu(111) surface partially covered by a defective Cu_2O(111) oxide exposing locally the Cu(111) surface, was used. We show that MBI has the ability to interact with the different local zones of the partially de-passivated surface. Therefore, it is a good candidate to enhance the barrier properties of de-passivated or incompletely passivated copper surfaces by healing the damaged oxide surface. The organic film is inhomogeneous, due to the difference in the adsorption configurations and adsorption strength of MBI on the different zones of the locally de-passivated surface (oxide and metal surfaces, oxide edges and oxide walls zones). Our results show similar adsorption configurations and interaction sites as for MBT, which can explain experimental results pointing to similar efficiency and behavior for MBT and MBI molecules to protect the copper from corrosion.

Computational Details

All calculations were performed by applying the framework of DFT with the periodic plane-wave basis set implemented in Vienna Ab initio Simulation Package (VASP).[24–27] All results reported have been obtained with projector-augmented-wave potentials using a 450 eV plane wave cutoff.[28,29] We used a Methfessel-Paxton smearing[30] with smearing value of 0.1 eV. Because of the large unit cell size used in calculations, the Brillouin zone sampling was restricted to the Γ-point.[31] We considered a non local correlation functional scheme proposed by Dion et al.[32] and Klimeŝ et al.[33–35] and calculations were carried out using OptB86b-vdw level,[34] offering a good compromise for the lattice parameters of bulk Cu-metal and Cu_2O-oxide[36,37] with equilibrium values of 3.599 (−0.30%) and 4.272 Å (+0.05%), in good agreement with experimental values of 3.61[38] and 4.27 Å,[39], respectively. Atomic positions were relaxed with the conjugate gradient (CG) algorithm until forces on each moving atom were less than 0.02 eVÅ^{-1}. All calculations are done without any constraint on the structure, except for the two bottom layers of the metals (asymmetric slab). The oxide and two upmost metal layers and the molecules were let free to relax. The vacuum region was set at more than 18 Å to minimize the interactions in the z direction between periodic images of the system.

The adsorption energy of the MBI molecule under thione (MBIH) and thiolate (MBI°) forms was calculated as:

$$E_{ads} = [E(\text{slab/MBI}) - E(\text{slab}) - nE(\text{MBI})]/n \quad [1]$$

where E(slab/MBI) is the total energy of the system with MBIH or MBI° adsorbed on the slab surface. E(slab) and E(MBI) are the energies of the bare, relaxed Cu(111)|| Cu_2O(111) slab and the free MBIH or MBI° molecule optimized in vacuum, respectively. n is the number of molecules on the surface.

When two configurations i and j are energetically compared, we use the total energy difference $\Delta E = E(i)–E(j)$ as well as the average energy difference (per molecule) $\Delta E_{ads}=E_{ads}(i)–E_{ads}(j)$, where E(i) and E(j) are the total energies, and $E_{ads}(i)$ and $E_{ads}(j)$ are the average adsorption energies of configurations i and j, respectively.

In order to analyze the local reactivity of different zones on the partially oxide-covered copper surface toward the MBI molecule, we calculated the local energetic trends of MBI on different surface zones as:

$$E^{*}_{ads} = -(E(\text{slab/MBI}_{n-1}) + E(\text{MBI}) - E(\text{slab/MBI}_{n})) \quad [2]$$

where E(slab/MBI_n) and E(slab/MBI_{n-1}) correspond to the total energy of the n and $(n-1)$ molecules adsorbed on the slab surface, respectively.

We plotted the charge density difference expressed as follows:

$$\Delta\rho(\mathbf{r}) = \rho(\mathbf{r})_{\text{slab/mol}} - (\rho(\mathbf{r})_{\text{slab}} + \rho(\mathbf{r})_{\text{mol}}) \quad [3]$$

where $\rho(\mathbf{r})_{\text{slab/mol}}$ is the charge density distribution on the adsorbed system. $\rho(\mathbf{r})_{\text{slab}}$ and $\rho(\mathbf{r})_{\text{mol}}$ are the charge density distributions on the isolated slab and the molecule for the geometry after adsorption, respectively. The geometry of "slab" and "molecule" are the same as in "slab/mol" obtained after optimization.

Model of locally de-passivated Cu(111) surface.—Our aim in this study is to investigate the interaction mechanism of MBI in its thione and thiolate forms as organic corrosion inhibitor on an incompletely passivated or locally de-passivated copper surface. Indeed, the locally exposed copper metal is susceptible to initiation of localized corrosion by pitting in aggressive environments. This can occur when the passive film does not saturate the metal surface during its growth process, which corresponds to an incomplete passivation of the metal surface, or after the local breakdown of the passive film, which corresponds to the local de-passivation. Because of the presence of different local types of exposed surfaces with different reactivity, we can expect that the efficiency of the inhibitor molecules will depend on their local interaction on the different zones of partially oxide-covered copper surface. The corrosion inhibition mechanism may thus differ depending on the local bonding and adsorption capability of the molecules. Molecules that would fully heal the passivation defect would be best inhibitors.

In our previous works, we built and optimized through quantum chemical DFT calculations a model of Cu(111) surface fully covered by a Cu_2O(111) passivation oxide,[37] which was derived from experimental measurements.[40–43] The model was used to study, as function of the oxide thickness, the structural and electronic properties, the reactivity toward hydration, surface hydroxylation,[37] as well as to investigate the adsorption mechanisms of MBT[44] and MBI[23] molecules on the oxidized copper surface covered by an intact oxide film. Further, from this model of Cu(111) copper surface with an intact ultrathin oxide film, we built a model of a partially oxide-covered copper surface by creating holes in the ultrathin oxide.[45] In this case (Fig. 1), the surface exposes both the oxide and metal surfaces, as well as oxide edges and oxide walls in the interfacial zones between the metal and oxide. The system depicts well the different reactive zones of a passivated surface locally exposing copper metal which allows us to investigate the

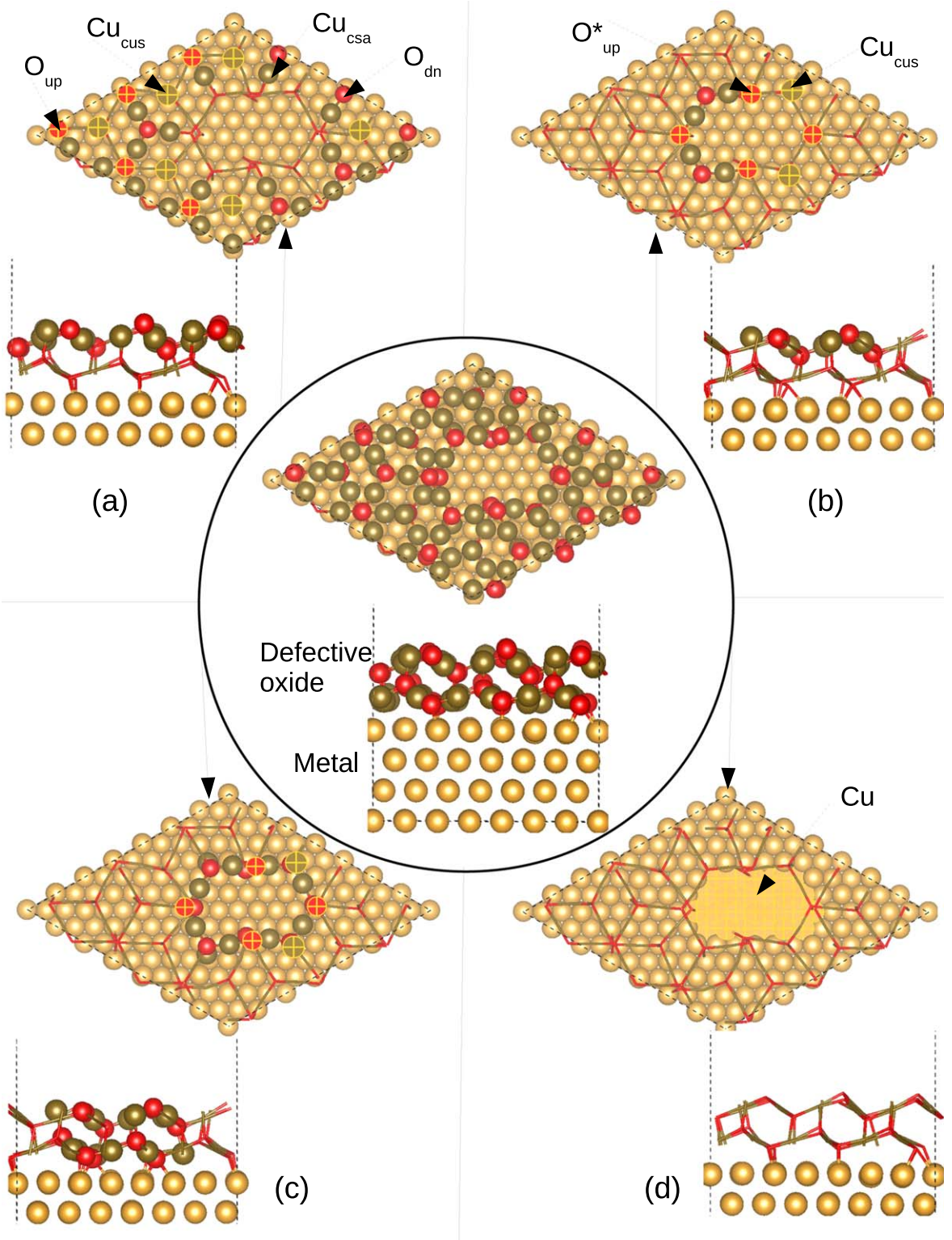

Figure 1. Cu(111) surface covered by ultrathin $Cu_2O(111)$ defective oxide. The reactive sites are shown in (a) for oxide surface, (b) for oxide edges, (c) for oxide walls and (d) for metal surface exposed by the defective oxide.

adsorption of the organic molecules on the different zones of the partially oxide-covered surface.

Here, we recall that the lateral dimensions of the supercell are 1.781 nm in both **a** ([1 $\bar{1}$ 0]) and **b** ([10 $\bar{1}$] or [01 $\bar{1}$]) with an angle of 60° or 120° between **a** and **b**, which corresponds to a (7×7) supercell of Cu(111) matching a (3 × 3) supercell of $Cu_2O(111)$ stoichiometric oxide. The supercell is composed by four Cu(111) layers covered by $Cu_2O(111)$ oxide, which consists of two O-Cu-O trilayers. After forming the hole in the oxide film (Fig. 1), the exposed oxide surface, oxide edges and oxide walls exhibit different copper and oxygen sites, namely two distinct copper sites labeled Cu_{csa} for coordinatively saturated and Cu_{cus} for coordinatively unsaturated Cu atoms and two distinct oxygen sites labeled O_{up} for unsaturated and O_{dn} for saturated oxygen atoms, where the

subscripts indicate the localized atom above (up) and below (dn) the surface Cu layer. In addition, the oxide edges contain doubly unsaturated oxygen sites labeled O^{*}_{up}, which are bonded to only two copper atoms. In contrast, O_{dn} and O_{up} atoms form four and three bonds with copper atoms, respectively. Finally, the metal Cu (111) surface exposes the metallic atoms, with the surface large enough for the MBI molecule to interact with different adsorption sites (atop, hollow (hcp and fcc) and bridge sites). The hole created in the oxide layer to mimic the local de-passivation has an area, 0.305 nm^2, corresponding to the area occupied by one molecule in the full organic monolayer formed on oxide-covered copper surfaces with an intact oxide film.

MBI Molecule.—Figure 2 depicts MBI molecules in thione (MBIH) and radical thiolate (MBI°) forms. The thiol form is not considered here. Indeed, according to literature, the thione form: i) is the preferred form in gaseous phase,[21,46] ii) has the highest reactivity in both vacuum and aqueous phases with thiolate form[47] and iii) is the dominant form in the crystal, which ensures the cohesion of the intermolecular N-H...S H-bonding network.[48] The physico-chemical properties of the MBI molecule for different species have been described in the literature using quantum chemical calculations.[17,22,49]

Using the same computational conditions as described above, we optimized the isolated molecules in a box (1 molecule/box) with dimensions of 20 Å × 20 Å × 20 Å in x, y, and z directions. For the radical MBI° form, the unrestricted spin was implemented to get the energy minimum. For better description of the adsorption configurations of MBI on the surface, we labelled the carbon atoms in the benzene ring with C_{3a} and C_{7a} being attached to the nitrogen N_3 and N_1, respectively. C_2 is the carbon atom in the hetero-cyclic ring shared between the two nitrogen and the sulfur atoms. We also represented the molecular plane and the molecular C_2 axis (axis joining the sulfur atom and the carbon C_2) to define the orientation of the molecule with respect to the surface plane.

Results and Discussion

As shown previously,[23] MBI can form a full monolayer on copper surfaces covered by an intact oxide film, with a density of 3.27 molecule/nm^2, meaning that each molecule can bond to one unsaturated Cu_{cus} site on the oxide surface. In the present work, focused on the surface chemistry of the organic monolayer formed by MBI molecules under thione and thiolate forms on copper surface covered by defective oxide film locally exposing the metal surface, we tried different adsorption configurations and searched for each one the most stable configuration on the passivation defect. In order to reduce the number of starting configurations, their constructions were based on our previous results obtained on the adsorption of MBI on copper surfaces covered by an intact oxide film[23] and on the bare metal surface.[22] On both surfaces at high coverage, the molecules (MBIH or MBI° species) adsorb with their planes perpendicular to the surface instead of the tilted and parallel orientations observed at low coverage. The molecules are oriented to the surface via the −S −NH termination for the thione form and via the −S −N termination for the thiolate form. Thus, in the present case, we considered initially only the perpendicular adsorption of the molecules with −S −NH termination (for thione) and the -S -N termination (for thiolate) oriented toward the different local surface zones.

The relevant configurations obtained for MBI adsorbed on the locally depassivated copper surface are shown in Figs. 3 and 4 for the thione and thiolate species, respectively. Each configuration contains 9 MBI (MBIH or MBI°) adsorbed molecules, which corresponds to high coverage with density of 3.27 molecule/nm^2. For the two configurations of MBIH shown in Figs. 3a and 3b, there are 6 molecules adsorbed on the oxide surface and 2 molecules on

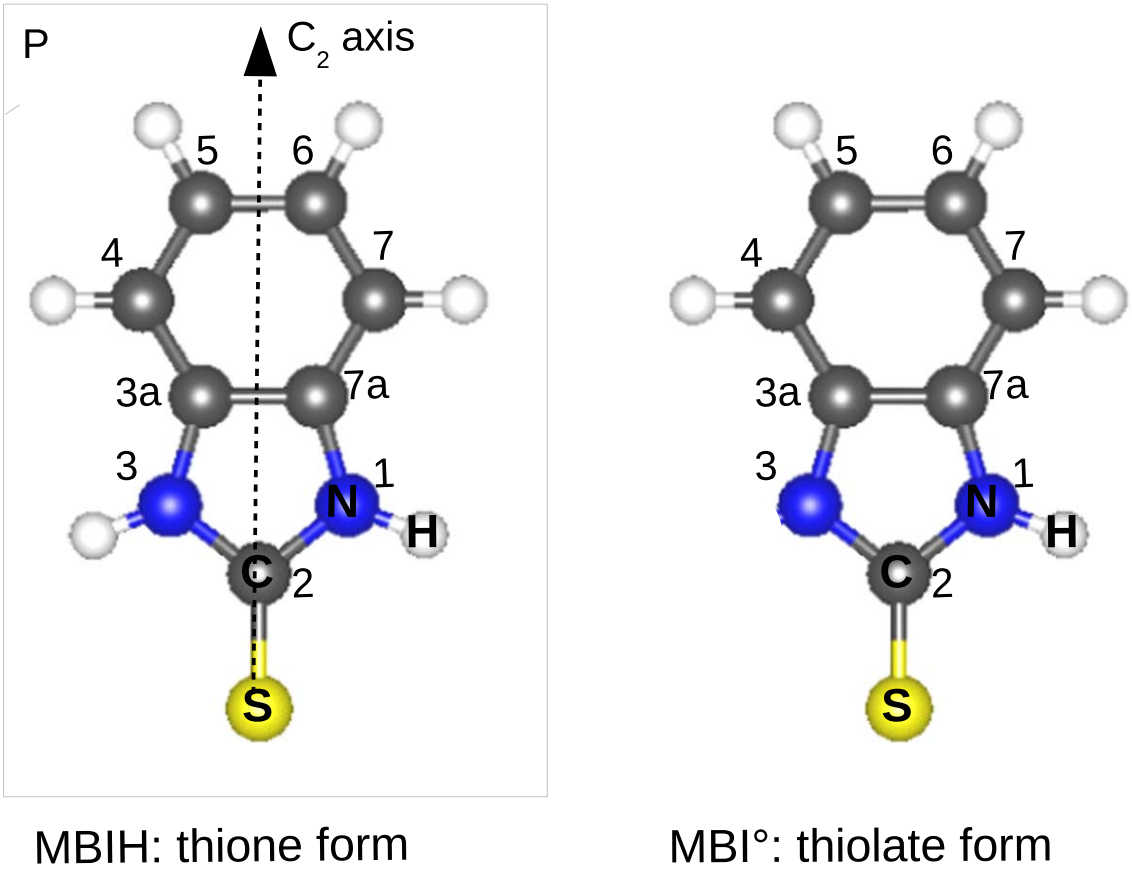

Figure 2. Thione (MBIH) and thiolate (MBI°) forms of MBI molecule. C_2 axis of the molecule joins the sulfur atom and the C_2 atom.

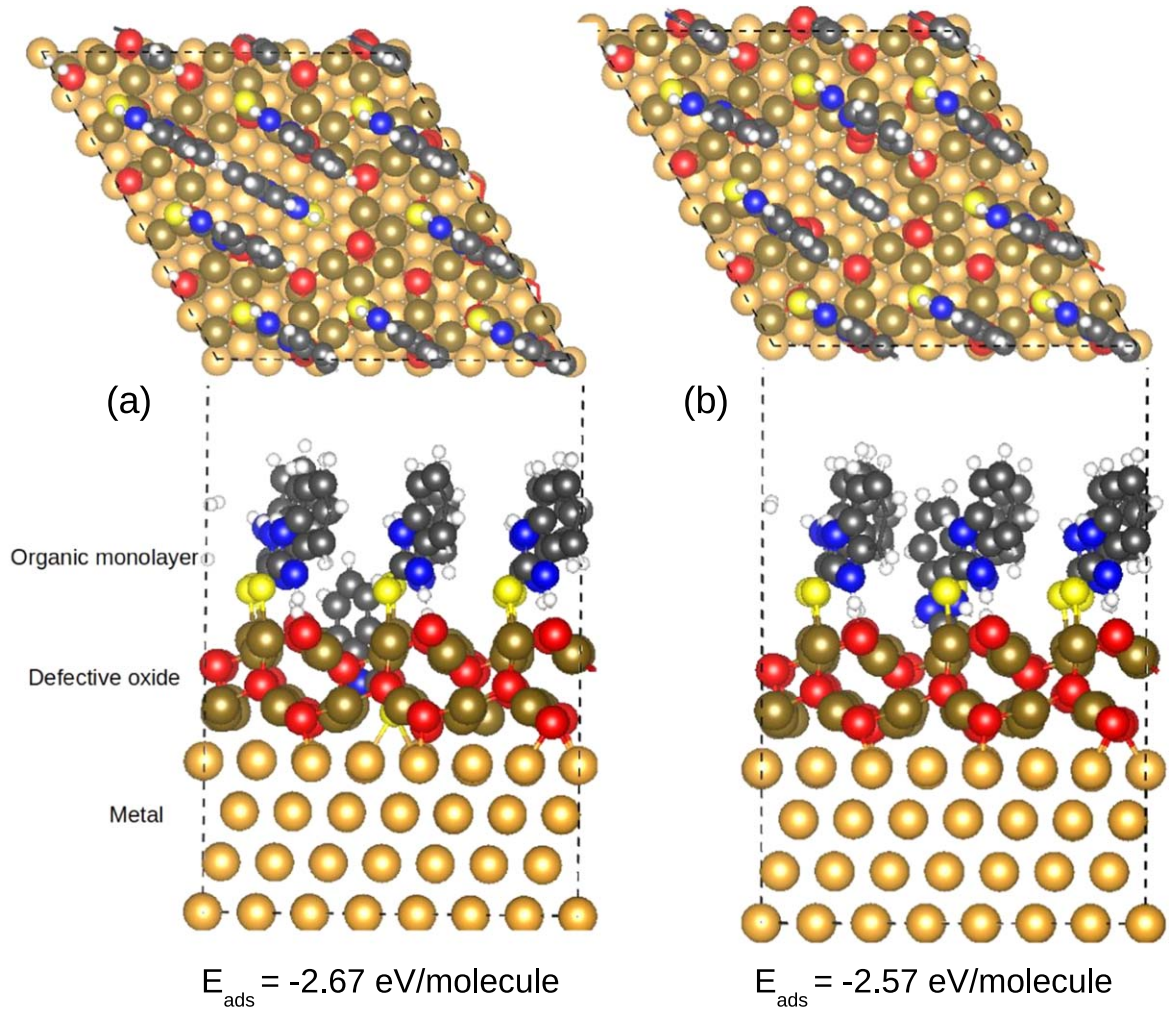

Figure 3. Side and top views of two most stable configurations (a) and (b) for the thione (MBIH) species adsorbed on the partially de-passivated copper surface (Cu(111) covered by Cu_2O(111) defective oxide).

the oxide edges zone. The difference between the two configurations is in the adsorption of the 9th molecule. It can be adsorbed on the metal at the bottom of the oxide hole (Configuration (a)) or on the oxide walls (Configuration (b)). In order to show better the dissimilarity in the adsorption configurations of the molecules according to the adsorption zone of the de-passivated copper surface, i.e. on the oxide and metal surfaces, on the oxide edges or on the oxide walls, we present in Figs. 5 the different snapshots for thione adsorbed on each local zone of the de-passivated copper surface. The snapshots (a) and (b) in Fig. 5 correspond to the molecules adsorbed on the oxide surface, the snapshot (b) is similar for the molecules adsorbed on the oxide edges, the snapshot (c) corresponds to the molecule adsorbed on the metal surface and the snapshot (d) to the molecule adsorbed on the oxide walls. For MBI°, the snapshot (a) in Fig. 6 is similar for all configurations shown in Fig. 4 for the molecules adsorbed on the oxide surface and on the oxide edges. It depicts the adsorption of 8 of the 9 molecules contained in the suppercell of the adsorbed layer. The differences between the different configurations in Fig. 4 relate to the adsorption of the 9th molecule depending on the local zone of the depassivated surface. They are depicted in snapshots (b) and (c) in Fig. 6. The 9th molecule is adsorbed on the metal surface in configuration (a) (see snapshot (b) in Fig. 6) or on the oxide walls in configurations (b) (see snapshot (c) in Fig. 6).

Energetic trends analysis.—It is well known that the adsorption energy and bonding strength of the molecules on the substrate surface determine their ability to form a protective organic film and thus their corrosion inhibition efficiency. The adsorption energies, calculated by Eq. 1, are reported together with the most stable configurations for the adsorbed thione and thiolate forms in Figs. 3 and 4, respectively. Regardless of the involved zone of the partially de-passivated copper surface and MBI species, the value of the adsorption energy is negative, meaning that the adsorption process is exothermic. This reveals the ability of both species to interact strongly with the different local surface zones and to form an organic layer on the surface. We calculated an average adsorption energy of −2.67 and −2.57 eV/molecule for the most stable configurations of MBIH shown in Fig. 3 (a) and (b), respectively. These values are less stable by 0.10 and 0.20 eV–molecule, respectively, than for the most stable MBIH configuration adsorbed on the copper surface covered by an intact oxide film (−2.77 eV/molecule),[23] indicating that, at same high surface coverage of 3.27 molecule/nm^2, MBIH is slightly less reactive toward the copper surface covered by a defective oxide film exposing locally the metal surface. For MBIH on the intact oxidized copper surface at high coverage we showed that about 13% of the adsorption energy ($E_{ads} = -2.72$ eV/molecule) is due to the lateral intermolecular contribution.[23] A similar contribution was calculated for the copper surface covered by the defective oxide, due to the similar density of the organic layer, where the lateral intermolecular contribution is about 11.4%. The slight difference in the contribution comes from the well-ordered organic layer formed on the intact oxidized copper surface, in contrast with the less ordered layer formed on the defective oxidized

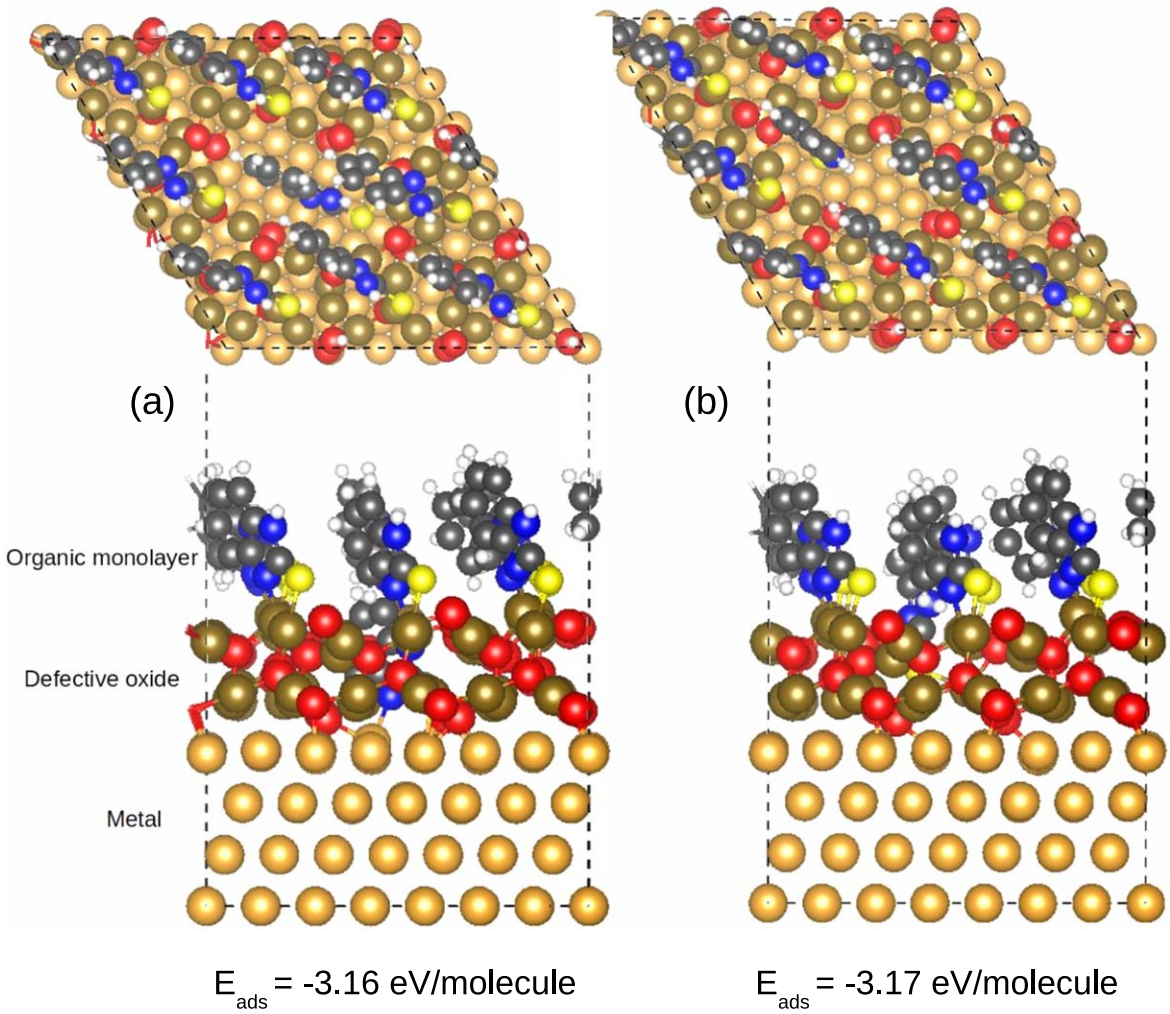

Figure 4. Side and top views of two most stable configurations (a) and (b) for the thiolate (MBI°) species adsorbed on the partially de-passivated copper surface (Cu(111) covered by Cu_2O(111) defective oxide).

surface. For MBI°, the adsorption energies for the most stable configurations shown in Fig. 4 (a) and (b) are −3.16 and −3.17 eV/molecule, respectively, considering thiolate species as energy reference. We obtained the following ranking in adsorption on oxidized copper surface at low coverage:[23] $MBI^{\circ}_{ads} + H_{ads}$ (−3.55 eV/molecule) is favoured over $MBIH_{ads}$ (−2.84 eV/molecule), which is favoured over $MBI^{\circ}_{ads} + \frac{1}{2} H_2$ (−2.61 eV/molecule). We thus concluded that the adsorption of MBI on the oxidized copper surface is favoured in the thiolate form (MBI°). The adsorption energies for all the configurations tested here are from 0.17 to 0.18 eV/molecule less negative than on the fully passivated copper surface (−3.34 eV/molecule)[23] indicating that, at the same coverage of 3.27 molecule/nm^2, MBI° is also less stable on the copper surface covered by a defective oxide film. In contrast, we found for MBT molecule that the adsorption energies are in the same range for adsorption on the copper surface covered by a defective oxide or by an intact oxide film with values around −2.70 and −3.10 eV/molecule for MBTH and MBT° species, respectively.[44,45]

The comparison of the formation of the organic film by MBI thione or thiolate species on different copper surface states reveals that both species can form dense organic films on oxide-free bare copper surfaces,[22] on copper surfaces covered by an intact oxide film[23] and also on copper surface covered by defective oxide film. However, the molecules adsorb less strongly on bare copper surfaces than on the fully passivated copper surfaces[23] and on partially de-passivated copper surfaces. On the bare Cu(111) surface, Vernack et al.[22] reported adsorption energy values of −0.86 and −1.42 eV/molecule for the thione form at coverage of 1.5 and 3.9 molecule/nm^2, respectively. For the thiolate conformer at the coverage of 1.5 molecule/nm^2, the adsorption energy is −1.25 and −2.60 eV/molecule, considering thione or thiolate forms as the reference for the adsorption energy calculation, respectively. Kozlica et al.[9] considered non-dissociative and dissociative adsorption mode of MBI (thione form) on O-covered and OH-covered Cu(111) surfaces, on O-terminated Cu_2O(111) surfaces and hydroxylated Cu_2O(111) surfaces. They found than that both the thione and thiolate species of adsorbed MBI can be expected on the different surfaces. The thione form is most favored on OH/Cu(111) and O-terminated Cu_2O(111) surfaces, with adsorption energies of −0.98 eV and −1.85 eV, respectively, whereas the thiolate form is most favored on O/Cu(111) and OH/ Cu_2O(111) surfaces, with adsorption energies of −1.85 eV and −1.21 eV, respectively, considering the thione form as the reference for the adsorption energy calculations. Geng et al.[50] showed that the adsorption of benzene thiolate on the bare (111) surface of metals including copper is the strongest, with an adsorption energy of −2.26 eV/molecule on Cu (111) surface. Still this value is inferior to what we found on the copper surface covered by a defective or intact oxide film. Note also that the adsorption of thiolate species from the dissociation of thione is an activated mechanism on copper surface covered by an intact oxide film, while it is without any activation energy on the oxide edge zones of the copper surface covered by defective oxide film, and consists of a spontaneous deprotonation of one NH group to

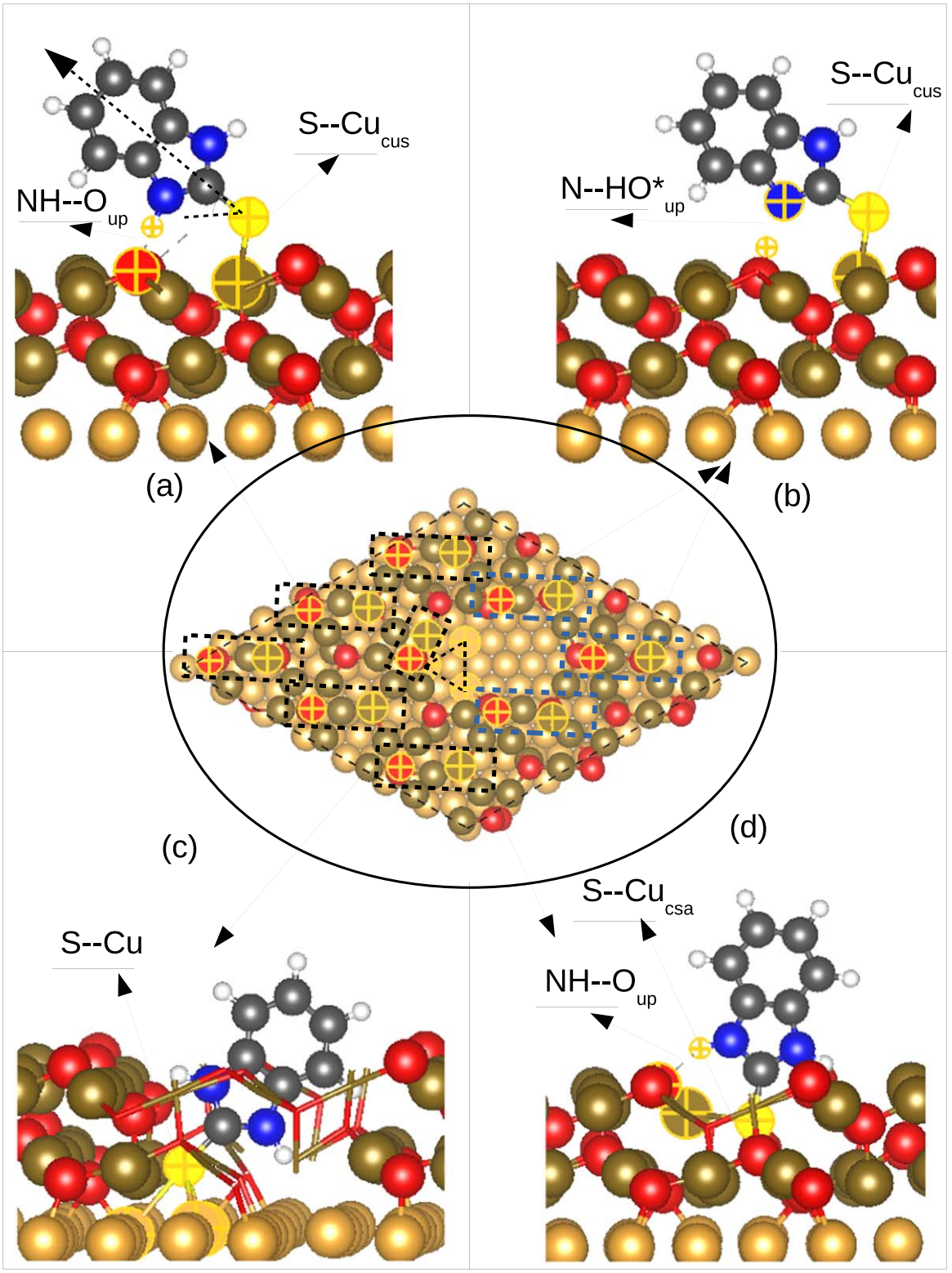

Figure 5. Snapshots of local adsorption configurations of MBIH form on the partially de-passivated copper surface. (a) on the oxide surface, (b) on the oxide edge, (c) on the metal surface and (d) on the oxide wall.

form OH group on oxide edge zones, due to the presence of doubly unsaturated sites.

This energetic analysis, based on the adsorption energy per molecule, reveals the average adsorption energy of the molecules in the organic layer and shows the ability of the MBI (and MBT) molecules to interact strongly with different copper surface states and to form dense organic layers. This quantity can also reflect the propensity of the molecules to form self-ordered monolayers (SAM) when the molecules are adsorbed on similar sites, because of the presence of symmetric adsorption sites like atop, bridge and fcc or hcp hollow sites on the bare Cu(111) surface and like Cu_{cus}, Cu_{csa} and O_{up} sites on the $Cu_2O(111)$ surface. However, the partially de-passivated copper surface exposes not only the sites of the Cu(111) and $Cu_2O(111)$ surfaces, but also different reactive sites at the oxide

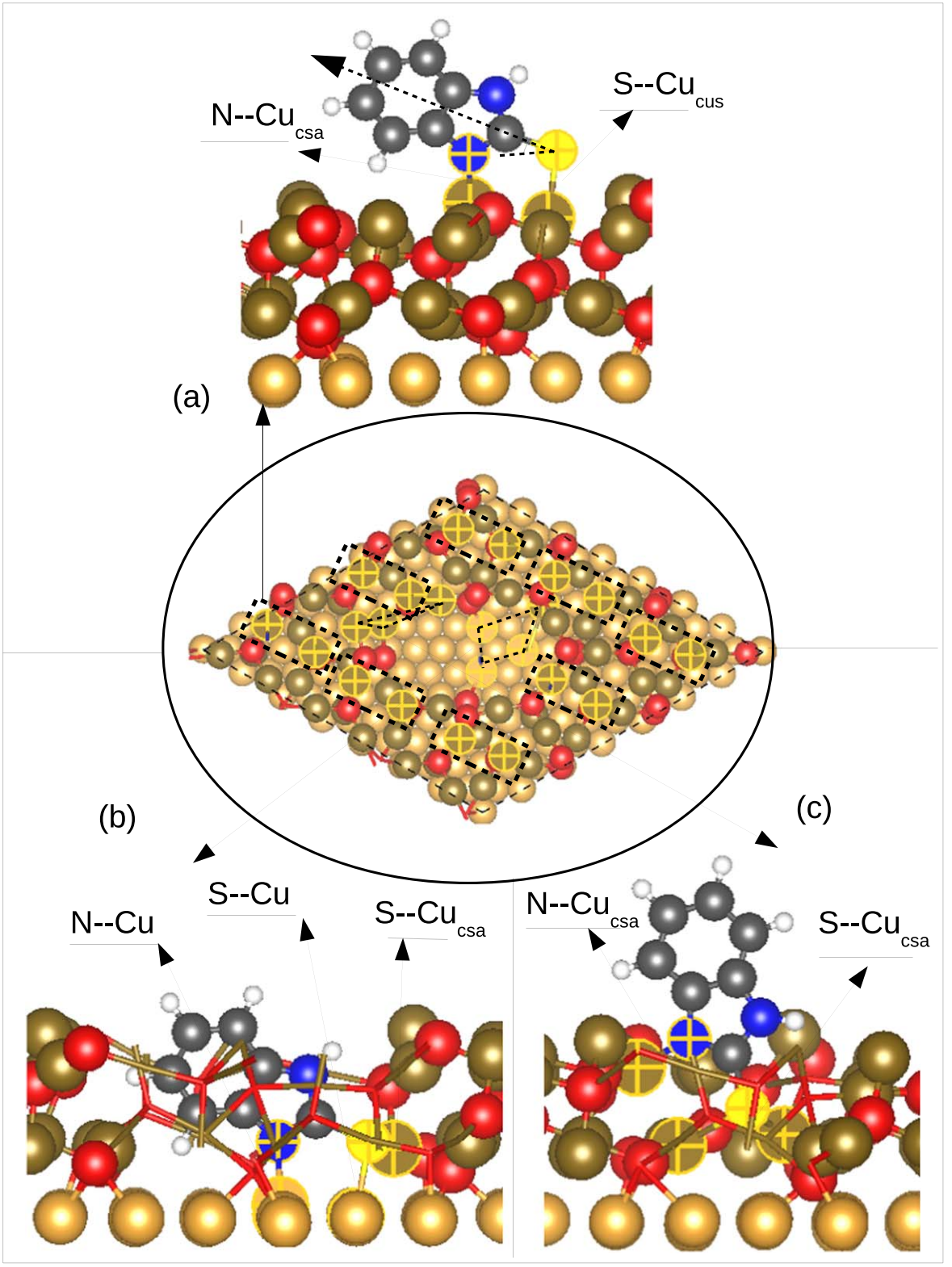

Figure 6. Snapshots of local adsorption configurations of MBI° form on the partially de-passivated copper surface. (a) on the oxide surface and oxide edge, (b) on the metal surface and (c) on the oxide wall.

edges and oxide walls. Thus, it is interesting to discuss the local energetic trends, in order to identify on which type of local surface zone the MBI molecule can interact in priority to form a dense organic monolayer on the partially de-passivated copper surface. Another important point to stress is the local adsorption configurations and the interaction mechanisms of the molecules, which also depend on the different local zones of the partially de-passivated surface as illustrated by Fig. 1. These details on the local adsorption energy and local adsorption configuration are discussed hereafter.

Local adsorption energy.—In order to investigate the local adsorption energy of the molecules in the dense organic monolayer,

we used Eq. (2) to calculate the adsorption energy of one molecule on each local zone of the partially de-passivated copper surface, which allows us to identify the most reactive parts of the surface by simple energy comparison. To do that, we started from the surface fully covered by the organic monolayer (9 molecules per supercell) and we removed one molecule from each part of interest of the partially de-passivated copper surface (leaving behind 8 molecules per supercell). We applied this protocol to all the different configurations of MBIH and MBI° shown in Figs. 3 and 4. The values of the local adsorption energy are compiled in Fig. 7 for MBIH and MBI° adsorbed on the different local zones of the partially de-passivated copper surface. They reveal that both forms of MBI interact strongly with the different zones. However, the local reactivity and the trend of the adsorption strength depend on the local zone of the surface involved in the interaction and on adsorbed configuration of the MBI species.

Comparative analysis reveals that the oxide edges are the most reactive toward the MBIH molecule adsorbed in dissociative form. They have the lowest adsorption energy, with a value of −3.11 eV. Spontaneous dissociative adsorption of MBIH occurs when the molecule is adsorbed on the oxide edges and also when it is shared between the oxide surface and the oxide edges, due to the combined presence of both unsaturated copper and doubly unsaturated oxygen sites localized on the oxide edges. We can expect that these uncoordinated sites are highly sensitive to corrosion due to faster dissolution and to preferential interaction with aggressive ions, like chlorides. However, as they are the favored sites for adsorption, the MBI molecules can block these corrosion mechanisms. The adsorption of MBIH on the oxide surface has an average energy of −2.77 eV making the oxide surface the second most reactive zone on the partially de-passivated copper surface. We recall that this surface zone contains similar adsorption sites as the intact oxide film (unsaturated copper and oxygen atoms) for adsorbing the MBIH molecule and that the molecules are adsorbed in intact form. The adsorption of the molecules on the oxide surface can thus enhance the chemical and/or physical barrier properties of the oxide film. The third most reactive local zone is the metal surface with an adsorption energy of −2.50 eV for MBIH. Even if this configuration is less stable by 0.61 eV compared to the oxide edges, the adsorption of the molecule remains exothermic. Thus, the molecule can fill the defective zone of the barrier oxide where the metal is exposed and protect the metal surface from interaction with the environment in the locally de-passivated zones. The fourth reactive local zone corresponds to the oxide walls, with an adsorption energy of −1.86 eV. In this local zone, the adsorption mechanism remains an exothermic process. Combining the adsorption on oxide walls and oxide edges, we can expect the inhibitor molecule to slow down the dissolution of the oxide and thus mitigate the enlargement of the de-passivated zones exposing the metal surface, which can limit and even stop the de-passivation process of the surface.

To summarize, the results for the thione form suggest that MBIH has the ability to interact with the different zones of a partially de-

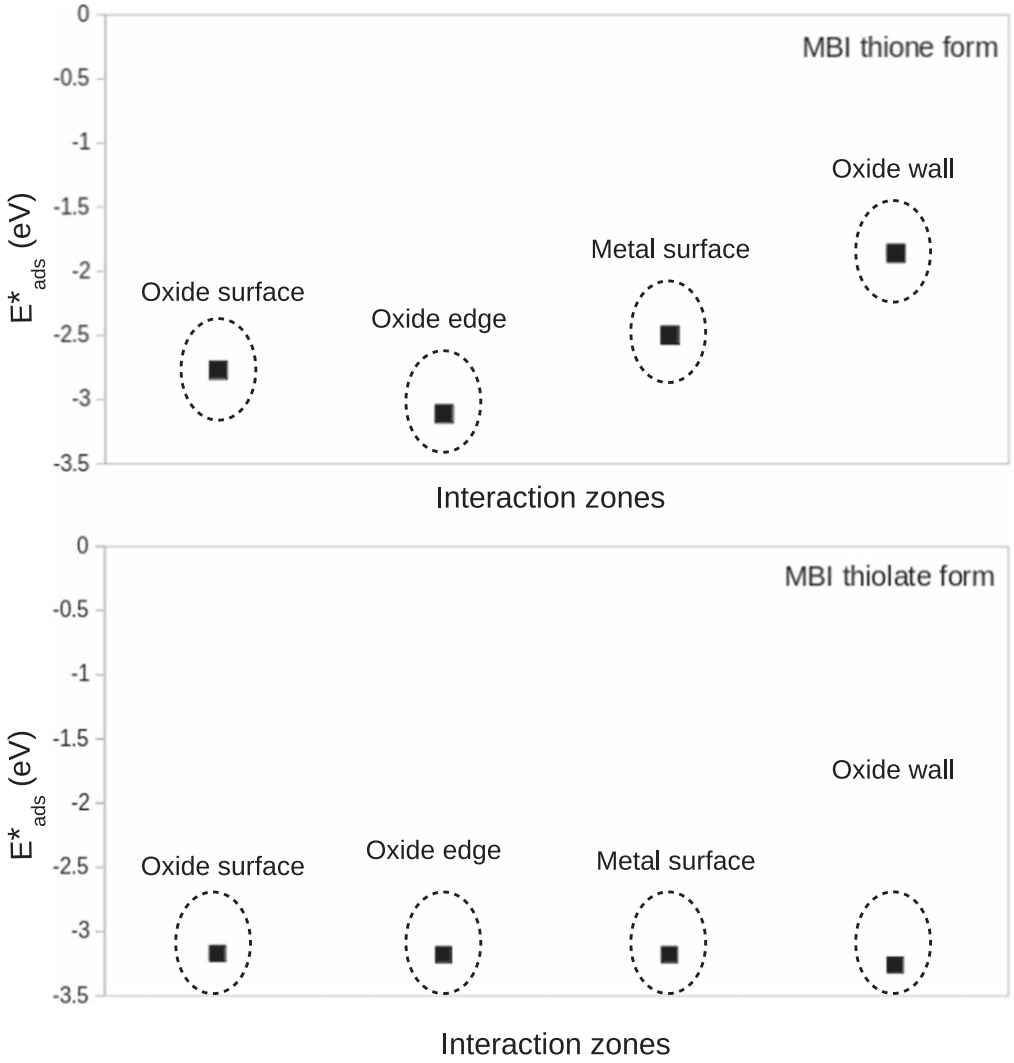

Figure 7. Local adsorption energy of thione and thiolate forms of MBI on different zones of the partially de-passivated copper surface (Cu(111) covered by Cu_2O(111) defective oxide).

passivated copper surface and can heal in priority the low coordinated sites, which are considered as more sensitive to the progress of de-passivation. The local adsorption strength increases as oxide walls < metal surface < oxide surface < oxide edges. In contrast, MBI° shows similar reactivity toward the different local zones of the partially de-passivated copper surface (Fig. 7). We calculated a local adsorption energy of −3.18 eV for the molecule adsorbed on the oxide surface, oxide edges and metal surface and an adsorption energy of −3.25 eV on the oxide walls. These values reveal no hierarchy between the local zones. The strong reactivity of these different local zones on the partially de-passivated surface toward MBI° adsorption also points to the ability of this conformer to protect the defective oxide film and to locally stop the de-passivation process. Note that the local adsorption energy behavior of the MBI inhibitor on the partially de-passivated copper surface is similar to that found for the MBT inhibitor molecule, except for the MBT thiolate form which has the lowest reactivity toward the oxide walls.[45] For thione form, MBT is more strongly bonded by about 0.25 eV/molecule than MBI on different de-passivated local zones. In contrast to thione form, the reactivity of MBI thiolate is stronger than that of MBT thiolate, where the local adsorption energy difference varies from 0.28 to 1 eV/molecule, according to the local adsorption zones. The similarity in the adsorption behavior of MBT and MBI organic inhibitors was also pointed out on the copper surface covered by an intact oxide film,[23,44] where MBT thione form is more strongly bonded by about 0.30 eV/molecule than MBI thione, conversely to thiolate form where MBI thiolate is more strongly bonded by 0.23 eV/molecule than MBT thiolate. The combined results show that both molecules are strongly bonded on the copper surface covered by an intact or defective passive oxide film and show similar adsorption configurations and interaction sites, which can explain experimental results pointing to similar efficiency and behavior for MBT and MBI molecules to protect copper from corrosion.

Local adsorption configurations for thione (MBIH) species.— MBIH adsorbed on the oxide surface presents two adsorption configurations shown in Fig. 5 (a) and (b). The configuration in snapshot (a) is similar to that found for MBIH adsorbed on the copper surface covered by an intact oxide film. The molecule is adsorbed in intact form with its plane perpendicular to the surface plane. The tilt angle of the molecular C_2 axis is about 35° with respect to the surface plane. The orientation of the molecule via -S and -NH terminations toward the Cu_{cus} and O_{up} atoms of the oxide surface favors its strong binding to the oxide surface. Indeed, MBIH covalently bonds via the S atom with the Cu_{cus} surface site and the binding is enhanced by the formation of a H–bond via one NH group with an O_{up} surface site. The bond length of S–Cu_{cus} is 2.17 Å and that of NH···O_{up} varies from 1.50 to 1.55 Å.

The configuration in snapshot (b) is observed on the oxide surface and on the oxide edges. The adsorption is dissociative and the molecule is oriented via -S and -N terminations to the surface. This adsorption mode requires the presence of an O^*_{up} site, which is localized on the oxide edge. On the oxide surface, there is also the implication of a Cu_{cus} site, while both O^*_{up} and Cu_{cus} sites are involved on the oxide edges. Therefore, the molecule can be considered as shared between the oxide edge and the oxide surface or only on the oxide edge. The dissociation is without any activation energy and it consists of spontaneous deprotonation of one NH group, the one that is directed to the surface and links with an O^*_{up} atom. This leads to the formation of an OH group on the oxide edge while MBIH deprotonates to MBI°. The molecular plane remains perpendicular to the surface, with a tilt angle of the C_2 axis of about 30°. The dissociatively adsorbed molecule binds covalently via its S atom to the Cu_{cus} site localized on the oxide surface or oxide edge zone. It also forms the H-bond via its N atom with the OH group (N···HO) formed after hydroxylation resulting from the deprotonation of the NH group, instead of an O···HN H-bond formed in intact non–dissociative adsorption configuration on the oxide surface. The bond lengths of S–Cu_{cus} and N···HO are 2.15 and 1.70 Å, respectively. We note that the intact and dissociative adsorption mechanisms were also observed for MBTH adsorbed on partially de-passivated copper surface.[45] In contrast, only the intact adsorption mechanism of MBIH and MBTH is favored on copper surfaces covered by an intact oxide film.[23,44]

Snapshot (c) in Fig. 5 corresponds to the most stable configuration of MBIH adsorbed on the metal surface exposed by the defective oxide. The molecule interacts with the copper metal only via its sulfur atom which corresponds to the -S orientation. Vernack et al.[22] reported that the adsorption of MBIH on the bare Cu(111) surface via -S or -S -NH terminations are isoenergetic ($\Delta E = 0.01$ eV). We find that the NH group is not involved in the interaction mechanism on the metal surface, in contrast to the oxide surface, oxide edges and oxide walls where the molecule can form NH···O or N···HO H-bonds. The molecular plane is perpendicular to the surface plane, with the molecular C_2 axis forming a tilt angle of 45° with respect to the surface plane. Thus, MBIH is adsorbed through the S atom on hcp hollow site of copper metal surface, with S–Cu bond lengths of 2.38, 2.50 and 2.55 Å. We noted that for MBTH, the S_{exo} and S_{endo} atoms can be adsorbed on close to bridge site and atop site, respectively, on the metal surface exposed by the defective oxide.[45] Indeed, the sulfur and the sulfur-containing molecules show a versatility of adsorption sites on Cu(111) surface, which allows the molecules to adapt and thus to form a dense organic monolayer, while ensuring a strong chemisorption of each molecule to the surface. The most stable sites on the bare Cu(111) surface is the hollow (fcc or hcp) site for atomic sulfur,[51] and for sulfur in MBT and MBI molecules at low coverage.[22] The adsorption configurations of MBIH on bare Cu(111) surface via S on fcc or hcp hollow sites are isoenergetic.[22] A combination of hollow and bridge sites is found at high coverage for MBT and MBI molecules.[22] However, on the Cu(111) surface covered by an intact Cu_2O(111) oxide, the sulfur of MBT and MBI molecules is adsorbed preferentially on top of Cu_{cus} site. The affinity of the nitrogen atom toward the copper is also demonstrated. The adsorption via one nitrogen atom can be accommodated on top sites for the interaction of the azoles and their derivatives on the bare Cu(111) surface.[18] For triazole the bonding via two nitrogen atoms on a bridge position is preferred at low coverage.[18]

MBIH adsorbed on the oxide walls (the walls resulting from the creation of a hole in the oxide film) is shown in snapshot (d) in Fig. 5. The most stable configuration corresponds to the molecular plane perpendicular to the surface plane and the molecule directed to the metal surface only via its sulfur atom (-S orientation). However, unlike for the adsorption configuration on the metal surface, one NH group is involved in the adsorption and it is directed toward the oxide wall. Now, the molecular C_2 axis is almost perpendicular to the surface plane (tilt angle is 85° meaning that the C_2 axis is almost parallel to the oxide wall surface). The S atom is at a distance of 3.85 Å from the metal surface. MBIH forms a covalent bond via the S atom with the Cu_{csa} surface site with a bond length of 2.59 Å. The binding of MBIH on oxide walls is also enhanced by the H-bonding via one NH group with an O_{up} surface site and the distance of NH···O_{up} is 1.82 Å.

Local adsorption configurations for thiolate (MBI°) species.— The adsorption of MBI° species is similar on the oxide surface and oxide edges and the adsorption configuration is shown in Fig. 6, snapshot (a). The molecule adopts -S -N orientation toward the surfaces and its molecular plane is almost perpendicular to the surface, tilt angle of the molecular C_2 axis is about 20° with respect to the surface plane. The orientation of the MBI° on the oxide surface and oxide edges toward Cu_{cus} to Cu_{csa} sites favors its strong binding by formation of two covalent bonds. The two covalent bonds are via the S and N atoms with the Cu_{cus} and Cu_{csa} sites, respectively. The bond lengths of S–Cu_{cus} and N–Cu_{csa} are 2.14 and 1.96 Å, respectively. This adsorption configuration is identical

to the configuration found for MBI° adsorbed on copper surfaces covered by an intact oxide film.[23]

The most stable configuration adsorbed on the metal surface at the bottom of the oxide hole is showed in Fig. 6, snapshot(b). The molecule is oriented perpendicularly to the surface with a tilt angle of the C_2 axis of 23° with respect to the surface plane. The S and N atoms (-S -N orientation) are directed toward the metal surface. This adsorption configuration via -S -N orientation is more stable by 0.29 eV than via -S -NH termination. MBI° is chemisorbed on the copper metal by the formation of two covalent bonds via the sulfur and nitrogen atoms. The S and N atoms are adsorbed on top and close to bridge copper sites, respectively, with S–Cu bond length is 2.28 Å and N–Cu bond lengths of 2.10 and 2.65 Å. MBI° also forms a third covalent bond via the S to Cu_{csa} of the oxide wall, with a S–Cu_{csa} bond length of 2.51 Å. In comparison, the MBT° thiolate species adsorbed on the metal surface of the partially de-passivated copper surface adopts different adsorption sites for the sulfur atoms.[45] The S_{exo} and S_{endo} atoms are close to bridge and top copper metal sites, respectively, for the -S -S orientation and S_{exo} is on bridge position for -S -N orientation. Vernack et al.[22] reported that, at high coverage of 3.9 molecule/nm^2 on the bare Cu(111) surface, MBI° is adsorbed perpendicularly and forms S–Cu and N–Cu covalent bonds. The sulfur atom in benzene thiolate was found more stable on fcc or bridge positions on bare metal surfaces, including on Cu(111).[50]

The most stable configuration of the MBI° conformer on the oxide walls is shown in Fig. 6, snapshot (c) and corresponds to -S -N orientation. The sulfur atom is oriented toward the surface, localized at a distance of 3.38 Å from the metal surface and does not bond to metal Cu atoms. The nitrogen atom is directed to the oxide wall. This -S -N orientation is more stable by 0.16 eV than the -S -NH orientation of MBI°, indicating that the molecule prefers the formation of a covalent bond via the -N atom rather than the formation of an H-bond via the NH group, thus enhancing its bonding strength to the oxide walls. MBI° binds covalently to the oxide wall via the S atom to two Cu_{csa} sites, with bond lengths of 2.20 and 2.70 Å. The deprotonated nitrogen atom also binds covalently to a Cu_{csa} site, with bond length of 1.95 Å. The Cu_{csa} sites involved in the adsorption mechanism are localized on the oxide walls. The molecular plane is perpendicular to the surface plane and the C_2 axis of the molecule has a tilt angle of 75° with respect to the surface plane.

Electronic analysis.—Analysis of the charge density difference ($\Delta\rho(\mathbf{r})$), was performed using Eq. 3 in order to confirm the types of bonds formed between the molecules and the substrate surfaces. Figures 8 and 9 show the $\Delta\rho(\mathbf{r})$ plots for different adsorption snapshots of MBIH and MBI°, respectively. For better visualization, only one molecule is shown in each case with an isosurface of 0.0004 e/Å^3 and 0.0009 e/Å^3 for the thione and thiolate species, respectively. In Fig. 8, snapshot (a) corresponds to MBIH adsorbed on the oxide surface in intact form and snapshot (b) corresponds to MBIH shared between the oxide surface and oxide edge in dissociative form (similar configuration on oxide edges). Snapshots (c) and (d) correspond to MBIH adsorbed on metal surface and oxide walls, respectively. For MBI° in Fig. 9, snapshot (a) corresponds to the molecule adsorbed on oxide surface and oxide edges, snapshot (b) to the molecule adsorbed on the metal surface and snapshot (c) to the molecule adsorbed on oxide walls. In Figs. 8 and 9, different values of the isosurfaces were selected for MBIH and MBI° in order to optimize the visualization of the $\Delta\rho(\mathbf{r})$ plots and the analysis of the bond formations. However, it precludes the comparative analysis of the bonding strength for MBIH and MBI° based on the $\Delta\rho(\mathbf{r})$ plots.

In Figs. 8 and 9, the formation of covalent bonds S–Cu and N–Cu is confirmed by charge density accumulation (light blue color) between the S and/or N atoms of the molecule and the Cu atom of the surface involved in the chemical interaction. H-bonding is confirmed by charge density accumulation on the O_{up} (light blue color) atom and charge density depletion (green color) on the hydrogen atom of the NH group in the intact adsorption configuration. In dissociative adsorption configuration of MBIH, H-bonding is evidenced by charge density accumulation on the N atom (light blue color) of the molecule and charge density depletion (green color) on the hydrogen atom of OH group. We recall that the H atom is dissociated from NH group and adsorbed on an O^*_{up} localized on the oxide edges, which leads to the formation of an OH group.

For MBIH adsorbed via -S -NH or -S -N orientation, strong bonding is confirmed by S–Cu_{cus} covalent bonding and NH$\cdots$$O_{up}$ or N$\cdots$$HO^*_{up}$ H-bonding on the oxide surface (Fig. 8a for intact adsorption and Fig. 8b for dissociative adsorption) and on the oxide edges (Fig. 8b). On the oxide walls (Fig. 8d), the electronic analysis evidences the S–Cu_{csa} covalent bonding and NH$\cdots$$O_{up}$ H-bonding. On the metal surface (Fig. 8c), MBIH is adsorbed only via the S atom toward the surface and the strong interaction is provided by S–Cu covalent bonding. The charge density difference for the adsorption of MBIH on the metal surface shows that the adsorption is enhanced by electrostatic interactions between one NH group and copper surface atom.

For MBI° adsorbed via -S -N oriented toward the oxide surface and oxide edges, strong bonding is confirmed by the formation of two covalent bonds, S–Cu_{cus} and N–Cu_{csa} as shown in Fig. 9a. On the metal surface, electronic analysis confirms that the molecule interacts via both S–Cu and N–Cu chemical bonding (Fig. 9b. On the oxide walls, the $\Delta\rho(r)$ plots confirm that the molecule interacts via S–Cu_{csa} and N–Cu_{csa} covalent bonding (Fig. 9c.

Conclusion

These DFT quantum chemical calculations bring atomic scale insight on the interaction mechanisms of the MBI organic inhibitor molecule on a partially de-passivated copper surface exposing locally the metal substrate. The reactive sites of the molecule are the S atom and NH group for the thione form and the S and N atoms for the thiolate conformer. The surface sites susceptible to interact with S and N (or NH) of the molecule are Cu_{cus} , Cu_{csa} (or O_{up}) on the oxide surface, Cu_{cus} and Cu_{csa} (or O^*_{up}) on the oxide edges, Cu_{csa} on the oxide walls and Cu on the metal surface. The comparison between MBT and MBI molecules show similar adsorption behavior involving similar reactive atoms of the surface, which can explain the similar mitigation brought by both molecules against the corrosion of copper observed experimentally in various conditions. Our results show the ability of the MBI molecule to adsorb strongly on a locally de-passivated or incompletely passivated copper surface. However, the adsorption mechanisms and the bonding strength depend both on the reacting conformer of MBI and the local adsorption zones of the copper surface covered by a defective passive oxide film.

The MBIH thione conformer binds via S–Cu_{cus} covalent bond and O$\cdots$HN H-bonding in intact form or OH$\cdots$N H-bonding in dissociative form on the oxidized surface and oxide edges of the de-passivated zone. The dissociative adsorption mechanism occurs spontaneously when the O^*_{up} doubly unsaturated oxygen site, localized on the oxide edges, is involved in the interaction mechanism. On the oxide walls of the de-passivated zone, MBIH forms S–Cu_{csa} covalent bond and O$\cdots$HN H-bond. On the metal surface, it forms one S–Cu covalent bond.

The MBI° thiolate conformer binds via two covalent bonds for the most stable configurations adsorbed on different zones of the locally de-passivated surface. It forms S–Cu_{cus} and N–Cu_{csa} bonds on the oxide surface and oxide edges. On the oxide walls, it forms S–Cu_{csa} and N–Cu_{csa} bonds, and it is adsorbed via S–Cu and N–Cu on the metal surface exposed by a defective oxide.

Our results show that the MBI molecule can form a dense organic monolayer strongly bonded to a partially de-passivated copper surface, with flexibility for local adsorption mode of the organic film. Increasing order of local adsorption strength for MBIH thione

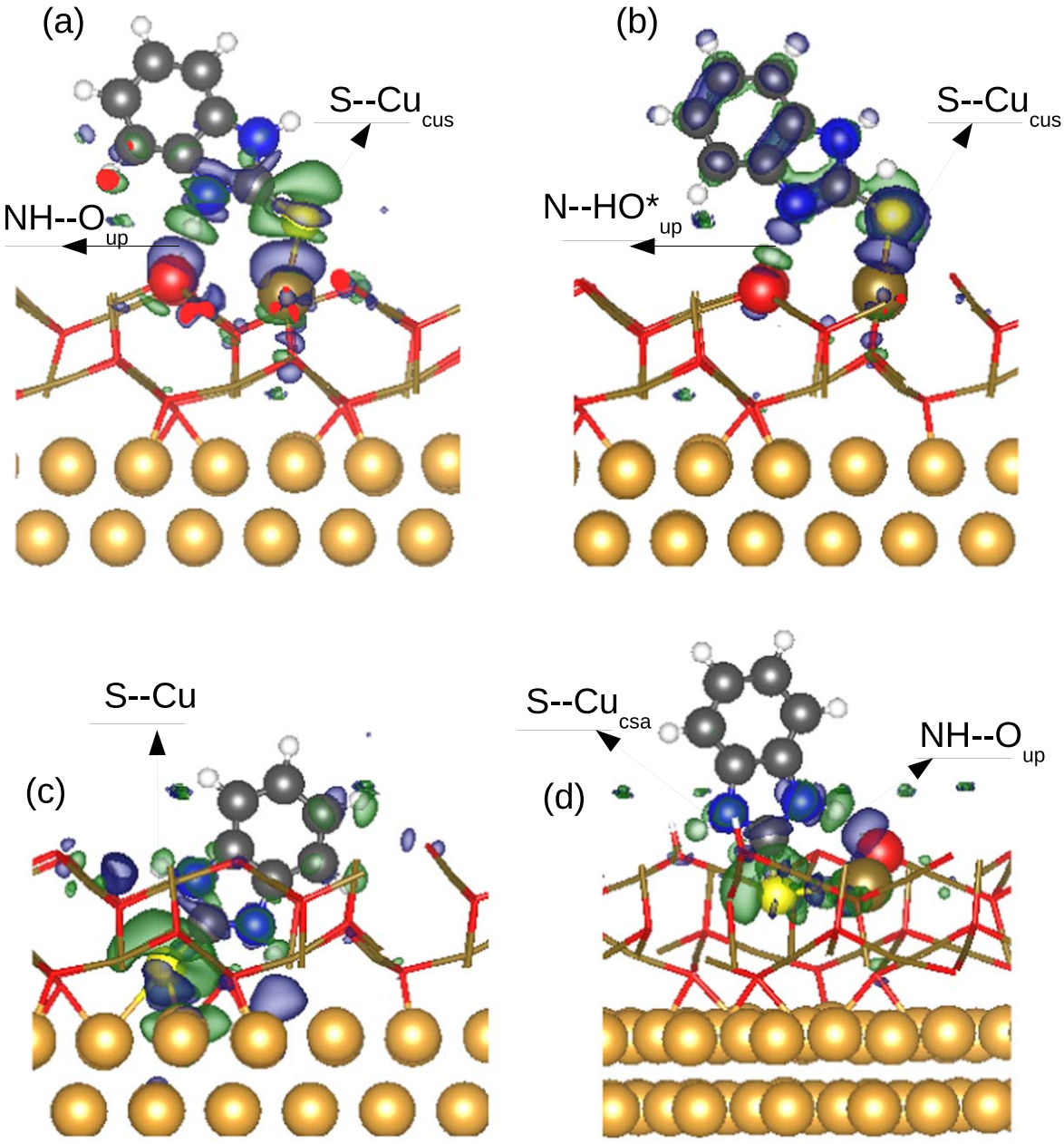

Figure 8. Charge density difference analysis for MBIH adsorbed on different zones of partially de-passivated copper surface. (a) on the oxide surface, (b) on the oxide edge, (c) on the metal surface and (d) on the oxide wall. Light blue color corresponds to accumulation of charge density and green color corresponds to depletion of charge density.

species is oxide walls < metal surface < oxide surface < oxide edges. In contrast, MBI° species shows similar local adsorption strength, independently of the reacting zones of the partially de-passivated surface.

The strong adsorption of both MBI thione or thiolate species on the different local zones of the copper surface covered by a defective passive oxide locally exposing the metal surface and its ability to form a dense organic film reveal that the molecule is an efficient organic inhibitor, including for protection of locally de-passivated or incompletely passivated copper surfaces. The molecule can simultaneously enhance the barrier properties of the passive oxide-covered surface and protect the uncovered metal surface exposed by local de-passivation or incomplete passivation. It can block the enlargement of the de-passivated zone by protecting the oxide edges and walls from dissolution as well as block the initiation of localized corrosion (pitting) by mitigating the dissolution of the bare metal in the de-passivated zone.

The combined results of MBT and MBI molecule inhibitors evidenced their ability to form protective films on copper surfaces covered by an intact or defective passive oxide film, which can explain their efficiency to mitigate the corrosion of copper in various conditions. The similar reactivity of both molecules toward the copper surface explains also their similar efficiency against corrosion observed experimentally.

Acknowledgments

This project has received funding from the European Research Council (ERC) under the European Union's Horizon 2020 research and innovation program (ERC Advanced Grant No. 741 123, Corrosion Initiation Mechanisms at the Nanometric and Atomic Scales: CIMNAS).

The authors thank GENCI for high performance calculations in the national (CINES) center under the A0040802217.

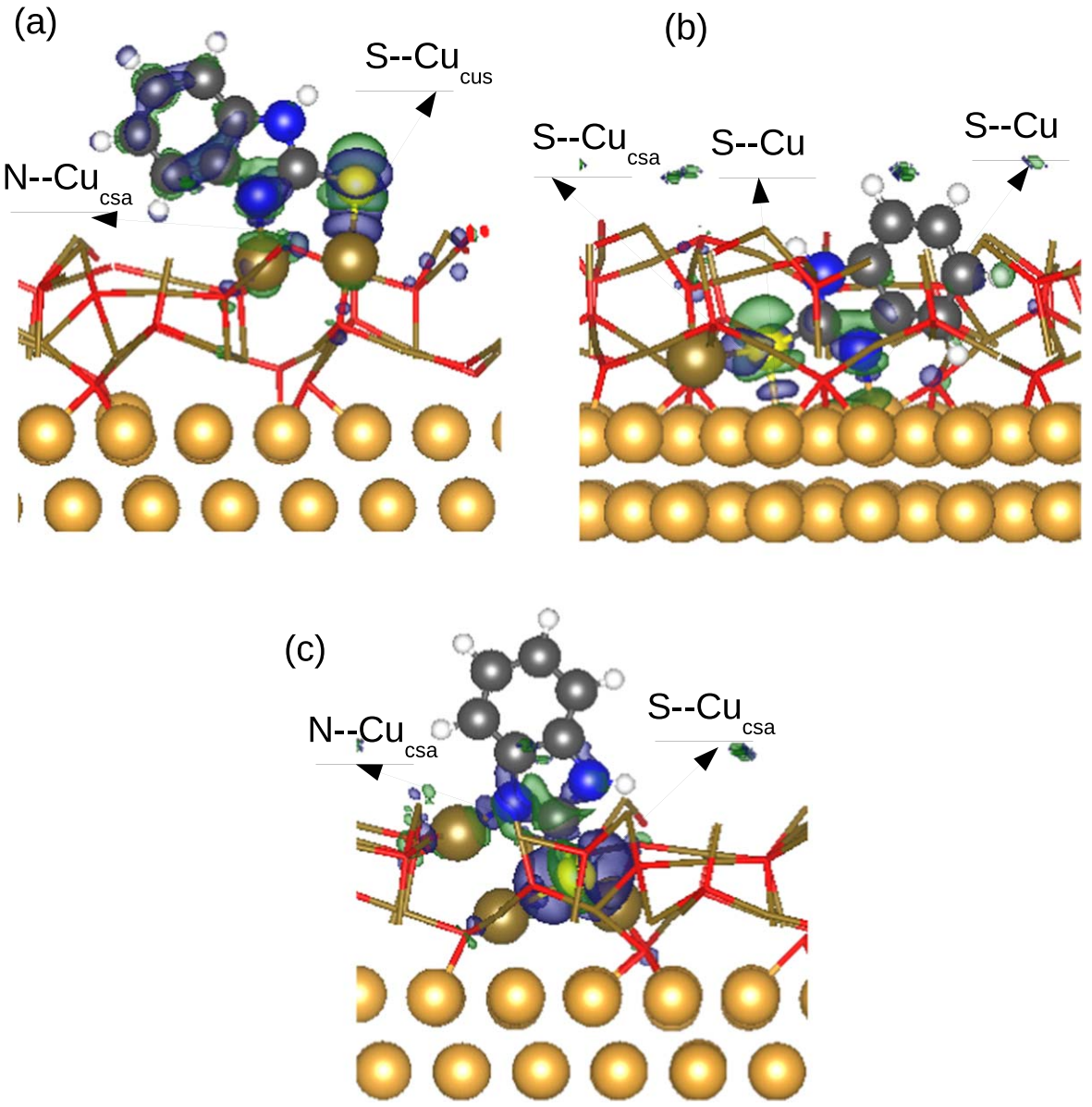

Figure 9. Charge density difference analysis for MBI° adsorbed on different zones of partially de-passivated copper surface. (a) on the oxide surface and oxide edge, (b) on the metal surface and (c) on the oxide wall. Light blue color corresponds to accumulation of charge density and green color corresponds to depletion of charge density.

ORCID

Dominique Costa https://orcid.org/0000-0002-3781-9867
Vincent Maurice https://orcid.org/0000-0001-5222-9972
Philippe Marcus https://orcid.org/0000-0002-9140-0047

References

1. D. Chadwick and T. Hashemi, "Electron spectroscopy of corrosion inhibitors: Surface films formed by 2-mercaptobenzothiazole and 2-mercaptobenzimidazole on copper." *Surf. Sci*, **89**, 649 (1979).
2. M. Finšgar, "2-Mercaptobenzimidazole as a copper corrosion inhibitor: Part I. Long-term immersion, 3D-profilometry, and electrochemistry." *Corros. Sci.*, **72**, 82 (2013).
3. I. Milošev, N. Kovačević, J. Kovač, and A. Kokalj, "The roles of mercapto, benzene and methyl groups in the corrosion inhibition of imidazoles on copper: I. Experimental characterization." *Corros. Sci.*, **98**, 107 (2015).
4. G. Žerjav and I. Milošev, "Protection of copper against corrosion in simulated urban rain by the combined action of benzotriazole, 2-mercaptobenzimidazole and stearic acid." *Corros. Sci.*, **98**, 180 (2015).
5. M. M. Musiani and G. Mengoli, "An electrochemical and SERS investigation of the influence of pH on the effectiveness of some corrosion inhibitors of copper." *J. Electroanal. Chem.*, **217**, 187 (1987).
6. P. M. Niamien, F. K. Essy, A. Trokourey, A. Yapi, H. K. Aka, and D. Diabate, "Correlation between the molecular structure and the inhibiting effect of some benzimidazole derivatives." *Mater. Chem. Phys.*, **136**, 59 (2012).
7. T. Shahrabi, H. Tavakholi, and M. G. Hosseini, "Corrosion inhibition of copper in sulphuric acid by some nitrogen heterocyclic compounds." *Anti-Corros. Methods Mater.*, **54**, 308 (2007).
8. J. Izquierdo, J. J. Santana, S. González, and R. M. Souto, "Scanning microelectrochemical characterization of the anti-corrosion performance of inhibitor films formed by 2-mercaptobenzimidazole on copper." *Prog. Org. Coat*, **74**, 526 (2012).
9. D. K. Kozlica, A. Kokalj, and I. Milošev, "Synergistic effect of 2-mercaptobenzimidazole and octylphosphonic acid as corrosion inhibitors for copper and aluminium—An electrochemical, XPS, FTIR and DFT study." *Corros. Sci.*, **182**, 109082 (2021).
10. F. X. Perrin and J. Pagetti, "Characterization and mechanism of direct film formation on a Cu electrode through electro-oxidation of 2-mercaptobenzimidazole." *Corros. Sci.*, **39**, 0536 (1998).
11. B. Trachli, M. Keddam, H. Takenouti, and A. Srhiri, "Protective effect of electropolymerized 2-mercaptobenzimidazole upon copper corrosion." *Prog. Org. Coat*, **44**, 17 (2002).
12. G. J. D. Xue, X. Y. Huang, and J. Zhang, "The formation of an effective anti-corrosion film on copper surfaces from 2-mercaptobenzimidazole solution." *J. Electroanal. Chem. Interfacial Electrochem*, **310**, 139 (1991).

13. D. Zhang, L. xin Gao, and G. ding Zhou, "Inhibition of copper corrosion in aerated hydrochloric acid solution by heterocyclic compounds containing a mercapto group." *Corros. Sci.*, **46**, 3031 (2004).
14. Sagar B. Sharma and L. H. K. Vincent, "Maurice; Marcus, P. Local Effects of Organic Inhibitor Molecules on Passivation of Grain Boundaries Studied In Situ on Copper." *J. Electrochem. Soc.*, **168**, 061501 (2021).
15. X. Wu, F. Wiame, V. Maurice, and P. Marcus, "Molecular scale insights into interaction mechanisms between organic inhibitor film and copper." *npj Materials Degradation*, **5**, 22 (2021).
16. M. Finšgar, "2-Mercaptobenzimidazole as a copper corrosion inhibitor: Part II. Surface analysis using X-ray photoelectron spectroscopy." *Corros. Sci.*, **72**, 90 (2013).
17. P. M. Niamien, H. A. Kouassi, A. Trokourey, F. K. Essy, D. Sissouma, and Y. Bokra, "Copper Corrosion Inhibition in 1 M HNO_3 by Two Benzimidazole Derivatives." *ISRN Mater. Sci.*, **2012**, 623754 (2012).
18. N. Kovačević and A. Kokalj, "Analysis of molecular electronic structure of imidazole- and benzimidazole-based inhibitors: A simple recipe for qualitative estimation of chemical hardness." *Corros. Sci.*, **53**, 909 (2011).
19. S. Sun, Y. Geng, L. Tian, S. Chen, Y. Yan, and S. Hu, "Density functional theory study of imidazole, benzimidazole and 2-mercaptobenzimidazole adsorption onto clean Cu(111) surface." *Corros. Sci.*, **63**, 140 (2012).
20. I. B. Obot, Z. M. Gasem, and S. A. Umoren, "Understanding the Mechanism of 2-mercaptobenzimidazole Adsorption on Fe (110), Cu (111) and Al (111) Surfaces: DFT and Molecular Dynamics Simulations Approaches." *Int. J. Electrochem. Sci.*, **9**, 2367 (2014).
21. N. Kovačević, I. Milošev, and A. Kokalj, "The roles of mercapto, benzene, and methyl groups in the corrosion inhibition of imidazoles on copper: II. Inhibitor-copper bonding." *Corros. Sci.*, **98**, 457 (2015).
22. E. Vernack, D. Costa, P. Tingaut, and P. Marcus, "DFT studies of 2-mercapto-benzothiazole and 2-mercaptobenzimidazole as corrosion inhibitors for copper." *Corros. Sci.*, **174**, 108840 (2020).
23. F. Chiter and D. Costa, "Maurice, V.; Marcus, P. Adsorption of 2-mercaptobenzimidazole Corrosion Inhibitor on Copper: DFT Study on Model Oxidized Interfaces." *J. Electrochem. Soc.*, **167**, 161506 (2020).
24. G. Sun, J. Kürti, P. Rajczy, M. Kertesz, J. Hafner, and G. Kresse, "Performance of the Vienna ab initio simulation package (VASP) in chemical applications." *J. Mol. Struct. THEOCHEM*, **624**, 37 (2003).
25. G. Kresse and J. Hafner, *Phys. Rev. B*, **47**, 558 (1993).
26. G. Kresse and J. Furthmüller, "Efficiency of ab-initio total energy calculations for metals and semiconductors using a plane-wave basis set." *Comput. Mater. Sci*, **6**, 15 (1996).
27. G. Kresse, "Furthm *ü* ller, J. Efficient iterative schemes for ab initio total-energy calculations using a plane-wave basis set." *Phys. Rev. B*, **54**, 11169–86 (1996).
28. G. Kresse and D. Joubert, "From ultrasoft pseudopotentials to the projector augmented-wave method." *Phys. Rev. B*, **59**, 1758 (1999).
29. P. E. Blöchl, "Projector augmented-wave method." *Phys. Rev. B*, **50**, 17953 (1994).
30. M. Methfessel and A. T. Paxton, "High-precision sampling for Brillouin-zone integration in metals." *Phys. Rev. B*, **40**, 3616 (1989).
31. H. J. Monkhorst and J. D. Pack, "Special points for Brillonin-zone integrations." *Phys. Rev. B*, **13**, 5188 (1976).
32. M. Dion, H. Rydberg, E. Schröder, D. C. Langreth, and B. I. Lundqvist, "Van der Waals Density Functional for General Geometries." *Phys. Rev. Lett.*, **92**, 246401 (2004).
33. J. Klimeš, D. R. Bowler, and A. Michaelides, "Chemical accuracy for the van der Waals density functional." *J. Phys.: Condens*, **22**, 022201 (2010).
34. J. Klimeš, D. R. Bowler, and A. Van der Michaelides, "Waals density functionals applied to solids." *Phys. Rev. B*, **83**, 195131 (2011).
35. J. Klimeš and A. Michaelides, "Perspective: Advances and challenges in treating van der Waals dispersion forces in density functional theory." *J. Chem. Phys.*, **137**, 120901 (2012).
36. F. Chiter, V. B. Nguyen, N. Tarrat, M. Benoit, H. Tang, and C. Lacaze-Dufaure, "Effect of van der Waals corrections on DFT-computed metallic surface properties." *Mater. Res. Express*, **3**, 046501 (2016).
37. F. Chiter, D. Costa, V. Maurice, and P. Marcus, "A DFT-based Cu(111)|| Cu_2O(111) model for copper metal covered by ultrathin copper oxide: structure, electronic properties and reactivity." *J. Phys. Chem. C*, **124**, 17048 (2020).
38. C. Kittel, *Introduction to Solid State Physics* (Wiley, New York, NY) 7th ed. ed. (1996).
39. A. Werner and H. D. Hochheimer, "High-pressure X-ray study of Cu20 and Ag20." *Phys. Rev. B*, **25**, 5929 (1982).
40. P. Marcus and V. Maurice, "Atomic level characterization in corrosion studies." *Phil. Trans. R. Soc*, **A375**, 20160414 (2016).
41. V. Maurice, H.-H. Strehblow, and P. Marcus, "In situ STM study of the initial stages of oxidation of Cu(111) in aqueous solution." *Surf. Sci*, **458**, 185 (2000).
42. J. Kunze, V. Maurice, L. H. Klein, H. H. Strehblow, and P. Marcus, "In Situ Scanning Tunneling Microscopy Study of the Anodic Oxidation of Cu(111) in 0.1 M NaOH." *J. Phys. Chem. B*, **105**, 4263 (2001).
43. J. Kunze, "Maurice, V.; Klein, L. H.; Strehblow, H.-H.; Marcus, P. In situ STM study of the duplex passive films formed on Cu(111) and Cu(001) in 0.1 M NaOH." *Corros. Sci.*, **46**, 245 (2004).
44. F. Chiter, D. Costa, V. Maurice, and P. Marcus, "DFT investigation of 2-mercaptobenzothiazole adsorption on model oxidized copper surfaces and relationship with corrosion inhibition." *Appl. Surf. Sci.*, **537**, 147802 (2021).
45. F. Chiter, D. Costa, V. Maurice, and P. Marcus, "Corrosion inhibition of locally depassivated surfaces by DFT study of 2-mercaptobenzothiazole on copper." *npj Materials Degradation*, **5**, 52 (2021).
46. A. L. R. Silva and M. D. M. C. R. da Silva, "Energetic, structural and tautomeric analysis of 2-mercaptobenzimidazole." *J Therm Anal Calorim*, **129**, 1679 (2017).
47. G. Liu, H. Zeng, Q. Lu, H. Zhong, P. Choi, and Z. Xu, "Adsorption of mercaptobenzoheterocyclic compounds on sulfide mineral surfaces: A density functional theory study of structure-reactivity relations." *Colloids and Surfaces A: Physicochem. Eng. Aspects*, **409**, 1 (2012).
48. K. Ravikumar, K. C. Mohan, M. Bidyasagar, and G. Y. S. K. Swamy, "Crystal structure of 2-mercaptobenzimidazole and bis[2- mercaptobenzimidazole]dichlorocobalt(II)." *J. Chem. Crystallogr*, **26**, 325 (1995).
49. G. A. Zhang, X. M. Hou, B. S. Hou, and H. F. Liu, "Benzimidazole derivatives as novel inhibitors for the corrosion of mild steel in acidic solution: Experimental and theoretical studies." *J. Mol. Liq.*, **278**, 413 (2019).
50. W. T. Geng, J. Nara, and T. Ohno, "Adsorption of benzene thiolate on the (111) surface of M (M=Pt, Ag, Cu) and the conductance of M/benzene dithiolate/M molecular junctions: a first-principles study." *Thin Solid Films*, **464-465**, 379 (2004).
51. C. R. B. Rodríguez and J. A. Santana, "Adsorption and diffusion of sulfur on the (111), (100), (110), and (211) surfaces of FCC metals: Density functional theory calculations." *J. Chem. Phys.*, **149**, 204701 (2018).